

# Analysis of the dynamic response of deep foundations with inclined piles by a BEM-FEM model

Luis A. Padrón, Juan J. Aznárez, Orlando Maeso and Ariel Santana

University Institute SIANI, Universidad de Las Palmas de G.C., Spain  
e-mail: {lpadron, jaznarez, omaeso, asantana}@iusiani.ulpgc.es

**Keywords:** Boundary element – finite element coupling, soil-structure interaction, inclined piles.

**Abstract.** A boundary element - finite element coupling formulation is used to address the dynamic behavior of deep foundations with inclined piles, modeling the soil by boundary elements as a three-dimensional zoned-homogeneous isotropic unbounded viscoelastic medium, and the piles by monodimensional finite elements as compressible Euler-Bernoulli beams. The problem is solved in the frequency domain. The formulation is briefly presented at the beginning of the paper. Then, validation results are presented for different foundation configurations and pile-soil stiffness ratios.

## Introduction

This work addresses the dynamic response of inclined piles and pile groups with inclined members, which are widely used in Civil Engineering but whose response under dynamic events has not been sufficiently analyzed up to date. In fact, their use in seismically active regions is discouraged by several building codes, even though there are some published results [1-3] suggesting that inclined piles may have beneficial rather than detrimental effects on the seismic response of foundation and superstructure.

A number of papers provide dynamic stiffness and damping functions of vertical piles but, up to the authors knowledge, impedance functions of inclined piles have been presented only by Giannakou et al. [4] and by Mamoon et al. [5], but for very few and specific cases. For this reason, and in order to contribute in this area, the methodology presented herein has been developed.

## Numerical Model

The boundary element method is used herein to model the dynamic response of the soil region taking into account the internal loads arising from the pile-soil interaction. These loads are modeled as distributions of tractions applied on a line defined by the pile axis, and are named 'load-lines'. On the other hand, the piles rigidity is introduced later into the system by using finite elements. The whole approach, together with the definition of the geometrical parameters of the problem, is depicted in Fig. 1.

Let the soil be considered as a linear, homogeneous, isotropic, viscoelastic, unbounded region  $\Omega$  with boundary  $\Gamma$ . The boundary integral equation for a time-harmonic elastodynamic state defined in the domain  $\Omega$  can be written in a condensed and general form as

$$\mathbf{c}^k \mathbf{u}^k + \int_{\Gamma} \mathbf{p}^* \mathbf{u} d\Gamma = \int_{\Gamma} \mathbf{u}^* \mathbf{p} d\Gamma + \sum_{j=1}^{n_p} \left[ \int_{\Gamma_{p_j}} \mathbf{u}^* \mathbf{q}^{s_j} d\Gamma_{p_j} + \Upsilon_j^k \mathbf{f}_{s_j} \right] \quad (1)$$

where  $\mathbf{c}^k$  is the local free term matrix at collocation point 'k',  $\mathbf{u}$  and  $\mathbf{p}$  represent the displacement and traction fields in the three directions of space,  $\mathbf{u}^*$  and  $\mathbf{p}^*$  are the elastodynamic fundamental solution tensors on the boundary  $\Gamma$  due to a time-harmonic concentrated load at point 'k',  $n_p$  is the number of piles, and  $\Gamma_{p_j}$  represents the pile-soil interface along the load-line  $j$ . In eq (1), the two terms between brackets represent the contribution of the internal loads, being  $\mathbf{q}^{s_j}$  and  $\mathbf{f}_{s_j}$  vectors containing the tractions (acting within the soil) along the pile-soil interface. More precisely,  $\mathbf{f}_{s_j}$  represents a point load placed at the tip of the pile, while  $\mathbf{q}^{s_j}$  is the distribution of interaction loads, along the pile shaft, applied on a line defined by the pile axis, both forces  $\mathbf{f}_{s_j}$  and  $\mathbf{q}^{s_j}$  coming from the pile-soil interaction along the different interfaces. On the other hand,  $\Upsilon_j^k$  represents the corresponding  $\mathbf{u}^*$  tensor computed at the tip of the pile. However, a singularity arises when the collocation point 'k' coincides with the tip node of the pile. In such a case, this term can be computed by considering the force at the tip of the pile as a vector of uniformly distributed tractions over a circular surface with radius  $R_p^2 = A/\pi$ , which yields a regular integral [6,7], being  $A$  the area of the pile section.

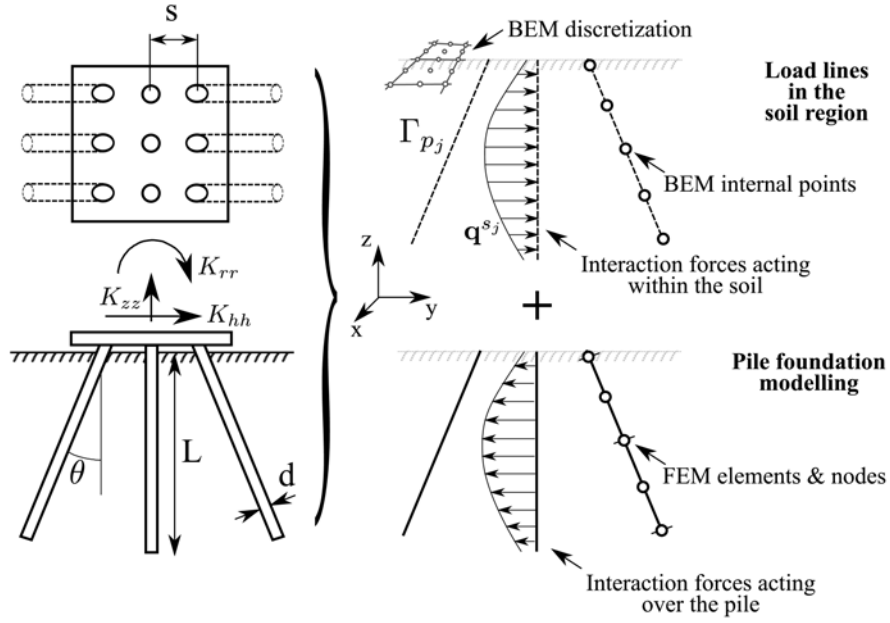


Figure 1. Pile foundation geometry and modeling through BEM-FEM coupling formulation

Following the usual procedure in the boundary element method, the numerical solution of eq (1) requires the discretization of the boundary surface. In this case, quadratic elements of six and nine nodes have been used. Then, over each boundary element, displacement and traction fields are approximated in terms of their values at nodal points ( $\bar{\mathbf{u}}$  and  $\bar{\mathbf{p}}$ ) making use of a set of polynomial interpolation functions [8]. The treatment of singularities can be found in [6,7].

Now, eq (1) can be written for all boundary nodes in  $\Gamma$  and all internal nodes in  $\Gamma_{pi}$ , yielding, respectively, the following two matrix equations

$$\mathbf{H}^{ss} \bar{\mathbf{u}} - \mathbf{G}^{ss} \bar{\mathbf{p}} - \sum_{j=1}^{n_p} \mathbf{G}^{sp_j} \bar{\mathbf{q}}^{s_j} - \sum_{j=1}^{n_p} \Upsilon_j^s \mathbf{f}_{s_j} = 0 \quad (2)$$

$$\bar{\mathbf{u}}^{p_i} + \mathbf{H}^{p_i s} \bar{\mathbf{u}} - \mathbf{G}^{p_i s} \bar{\mathbf{p}} - \sum_{j=1}^{n_p} \mathbf{G}^{p_i p_j} \bar{\mathbf{q}}^{s_j} - \sum_{j=1}^{n_p} \Upsilon_j^{p_i} \mathbf{f}_{s_j} = 0 \quad (3)$$

where  $\mathbf{H}$  and  $\mathbf{G}$  are coefficient matrices obtained by integration over the elements of the fundamental solution times the corresponding shape functions,  $\bar{\mathbf{u}}$  and  $\bar{\mathbf{p}}$  are the vectors of nodal displacements and tractions of the boundary elements, and  $\bar{\mathbf{u}}^{p_i}$  is the vector of nodal displacements along load-line  $i$ . On the other hand, piles are discretized using three-node beam elements with 13 degrees of freedom: three displacements on each node and two rotations at each of the ends. Linear axial deformation is allowed and pile flexural behavior is modeled according to the Euler-Bernoulli beam theory, but torsional response is not included in the model. After the discretization process, the dynamic behavior of pile  $j$  can be represented, in the finite-element sense, by a matrix equation

$$(\mathbf{K}_j - \omega^2 \mathbf{M}_j) \bar{\mathbf{u}}^{p_j} = \mathbf{f}_j^{ext} - \mathbf{Q}_j \bar{\mathbf{q}}^{s_j}, \quad (4)$$

where  $\omega$  is the circular frequency of excitation,  $\bar{\mathbf{u}}$  is the vector of nodal translation and rotation amplitudes along the pile,  $\mathbf{f}_j^{ext}$  includes the external forces acting at the top and the tip of the pile,  $\mathbf{K}_j$  and  $\mathbf{M}_j$  are the stiffness and mass matrices of the pile, and  $\mathbf{Q}_j$  is the matrix that transforms these nodal traction components to equivalent nodal forces. As usual, matrices  $\mathbf{K}_j$ ,  $\mathbf{M}_j$  and  $\mathbf{Q}_j$  are expressed herein as global matrices, obtained following the general assembly process of the finite element method from the elemental matrices defined for a general vertical element [6,7] and after pre and post multiplying by the corresponding rotation matrices in order to adapt to the pile inclination.

Now, imposing equilibrium and compatibility conditions along the load lines, and prescribing boundary conditions, eqs (2), (3) and (4) can be rearranged in a system of equations of the type

$$\mathbf{A} \{ \bar{\mathbf{u}}, \bar{\mathbf{p}}, \bar{\mathbf{q}}^s, \bar{\mathbf{u}}^p, \mathbf{f}_s \}^T = \mathbf{B} \quad (5)$$

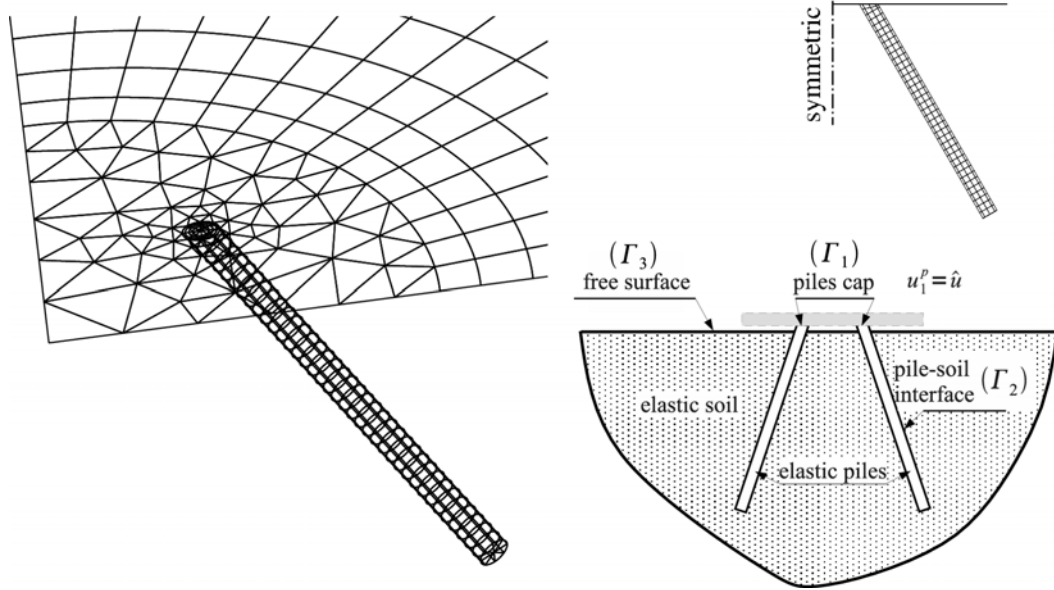


Figure 2. Multi-region boundary-element model definitions and BEM mesh details.

### Comparison Results

The formulation presented above was implemented in a previously existent multi-region BEM FORTRAN code [9, 10]. The aim of this section is the validation of this formulation (and its implementation) through a set of comparison results corresponding to dynamic stiffness and damping functions for  $2 \times 2$  pile groups. To this end, the computation of the dynamic stiffness and damping functions of pile groups is going to be validated against results from an advanced 3-D multi-region boundary element code for time-harmonic elastodynamic problems as presented in [9,10].

**3-D boundary element formulation.** In this multi-region boundary element formulation, both soil and piles are modeled as continuum isotropic homogeneous linear viscoelastic regions with their actual geometries. The boundary integral representation of the displacements in each domain (soil and each pile) corresponds to eq (1) but leaving the right hand side only with the first term. For the specific case of a single floating pile embedded in a viscoelastic half-space, the boundary element equations for each region (pile and soil) in partitioned form are:

$$\mathbf{H}_1^p \mathbf{u}_1^p + \mathbf{H}_2^p \mathbf{u}_2^p = \mathbf{G}_1^p \mathbf{p}_1 + \mathbf{G}_2^p \mathbf{p}_2 \quad (8)$$

$$\begin{bmatrix} \mathbf{H}_2^{pp} & \mathbf{H}_2^{ps} \\ \mathbf{H}_3^{sp} & \mathbf{H}_3^{ss} \end{bmatrix} \begin{bmatrix} \mathbf{u}_2 \\ \mathbf{u}_3 \end{bmatrix} = \begin{bmatrix} \mathbf{G}_2^{pp} & \mathbf{G}_2^{ps} \\ \mathbf{G}_3^{sp} & \mathbf{G}_3^{ss} \end{bmatrix} \begin{bmatrix} \mathbf{p}_2 \\ \mathbf{p}_3 \end{bmatrix} \quad (9)$$

corresponding eqs (8) and (9) to pile and soil regions, respectively. According to Fig. 2, sub-indexes 1 to 3 of the above equations correspond, respectively, to the pile connection with the rigid cap where nodal displacements are known ( $\Gamma_1$ ), to the pile-soil interface ( $\Gamma_2$ ), and to the soil free-traction ground surface ( $\Gamma_3$ ). Imposing, on the above expressions, external boundary conditions together with compatibility and equilibrium along the pile-soil interfaces, the combined equations for the coupled impedance problem can be written as

$$\begin{bmatrix} -\mathbf{G}_1^p & \mathbf{H}_2^p & \mathbf{G}_2^p & \mathbf{0} \\ \mathbf{0} & \mathbf{H}_2^{pp} & -\mathbf{G}_2^{pp} & \mathbf{H}_2^{ps} \\ \mathbf{0} & \mathbf{H}_3^{sp} & -\mathbf{G}_3^{sp} & \mathbf{H}_3^{ss} \end{bmatrix} \begin{bmatrix} \mathbf{p}_1^p \\ \mathbf{u}_2 \\ \mathbf{p}_2 \\ \mathbf{u}_3 \end{bmatrix} = \begin{bmatrix} -\mathbf{H}_1^p \hat{\mathbf{u}} \\ \mathbf{0} \\ \mathbf{0} \\ \mathbf{0} \end{bmatrix} \quad (10)$$

All boundaries (pile-soil interfaces, pile-cap interfaces and ground surface) are discretized into a finite number of quadratic nine-node and six-node boundary elements. Details of one of the used meshes in this work are shown in Fig. 2. Note that, due to the problem symmetries, only one quarter of the geometry needs to be discretized. This multi-region BEM code, being more rigorous and versatile than the simplified BEM-FEM coupling scheme presented before, presents clear disadvantages when it comes to performing parametric studies. Such disadvantages are all related to the relatively high number of degrees of freedom involved in a boundary-element

model and also to the amount of work needed to produce the mesh corresponding to each one of the configurations to analyze. Both negative aspects are clearly improved by the coupling formulation, where the number of degrees of freedom is radically reduced, and the pile discretization, much more simple to define, is independent of the soil mesh.

$\theta$	$10^\circ$	$20^\circ$	$30^\circ$
$s/d$	5	10	10

Table 1. Configurations used for validation of dynamic stiffness and damping functions.

**Validation results.** In this section, comparison results are shown for several configurations of  $2 \times 2$  inclined pile groups. Three different rake angles have been considered for these plots:  $\theta = 10^\circ$ ,  $20^\circ$  and  $30^\circ$ . The first case corresponds always to a pile separation ratio of  $s/d = 5$ , while the other two correspond to  $s/d = 10$ . Also, for  $\theta = 10^\circ$  and  $30^\circ$ , piles are always inclined parallel or perpendicular to the direction of excitation. On the other hand, the configuration used for  $\theta = 20^\circ$  corresponds to a case in which the piles are inclined, symmetrically, along the cap diagonals (see Table 1). Results are shown for the two different pile-soil stiffness ratios considered in this paper. Figs. 3 to 6 present horizontal, vertical, rocking and horizontal-rocking crossed dynamic stiffness and damping functions for the configurations described above. Results corresponding to the boundary element – finite element coupling formulation presented in this work are labeled as “BEM-FEM” and plotted using points, while those obtained from the multi-region boundary element code are labeled as “BEM-BEM” and plotted using solid lines. In the horizontal and rocking cases, results are provided for excitation modes along both horizontal axes. It can be seen that a very good agreement exists between the BEM-FEM coupling scheme used in the following section and the more rigorous boundary element code.

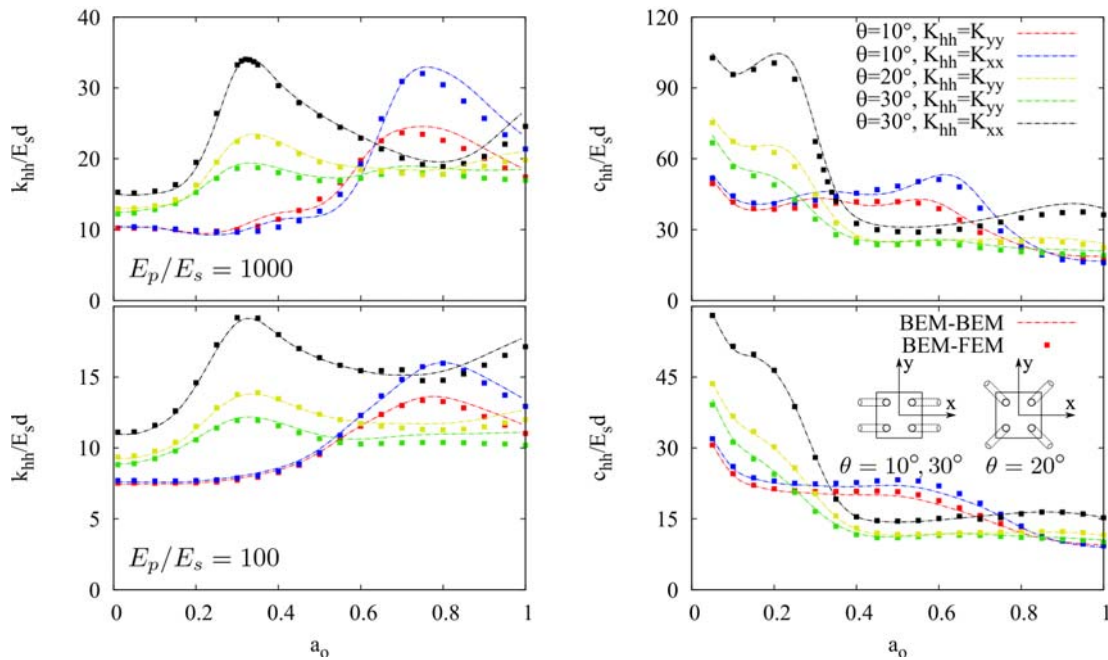


Figure 3. Comparison between horizontal impedances obtained by BEM-BEM and BEM-FEM models.

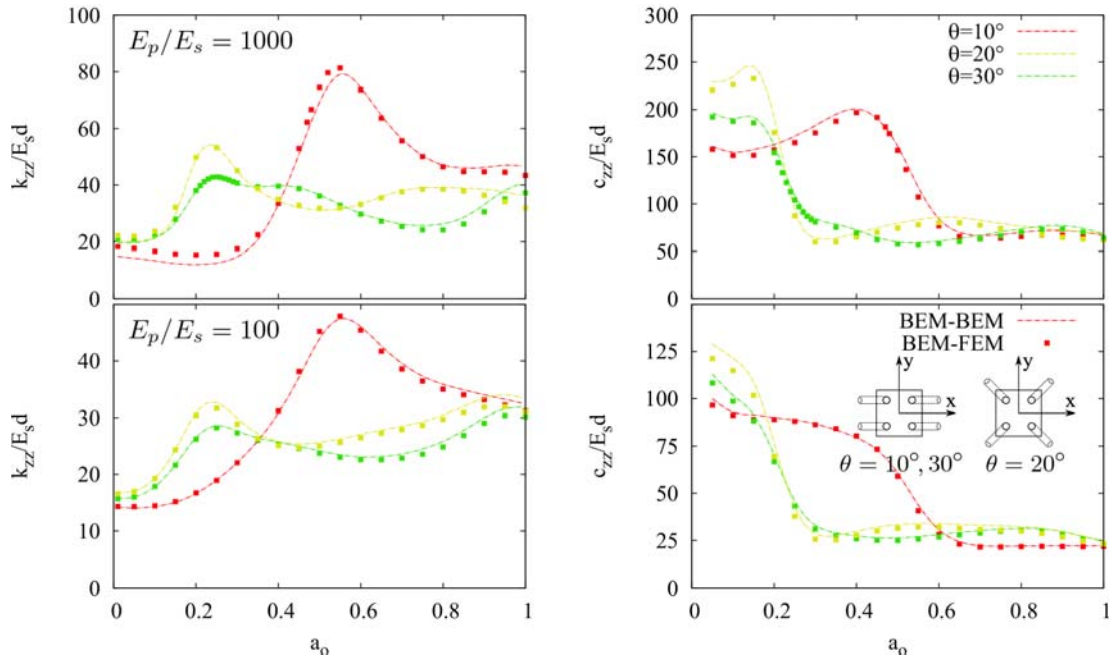


Figure 4. Comparison between vertical impedances obtained by BEM-BEM and BEM-FEM models.

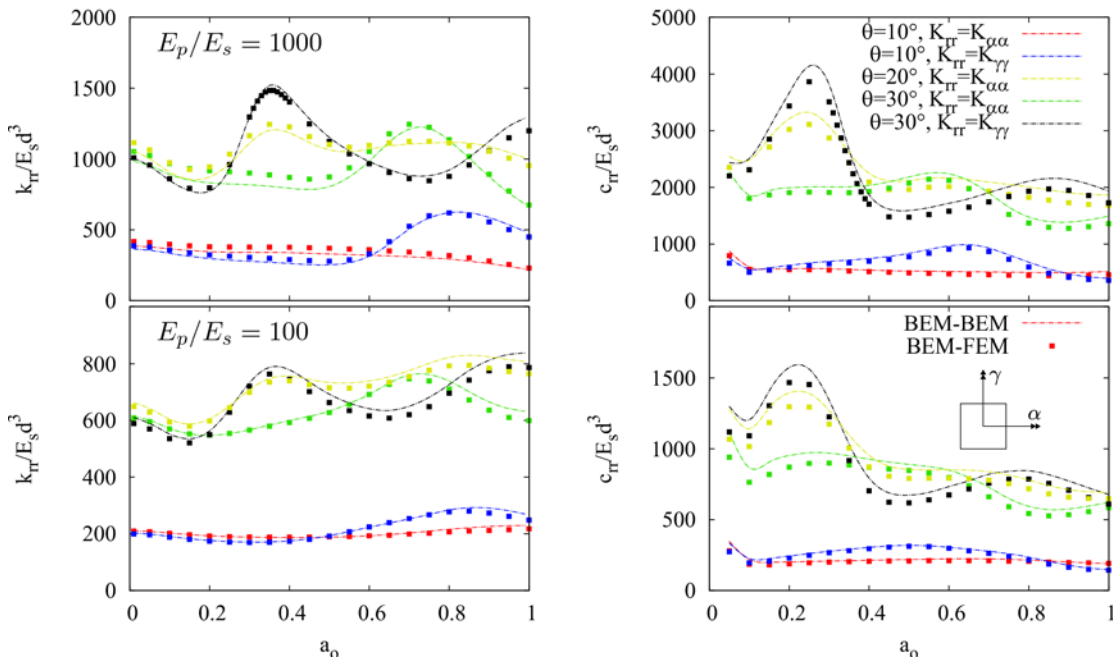


Figure 5. Comparison between rocking impedances obtained by BEM-BEM and BEM-FEM models.

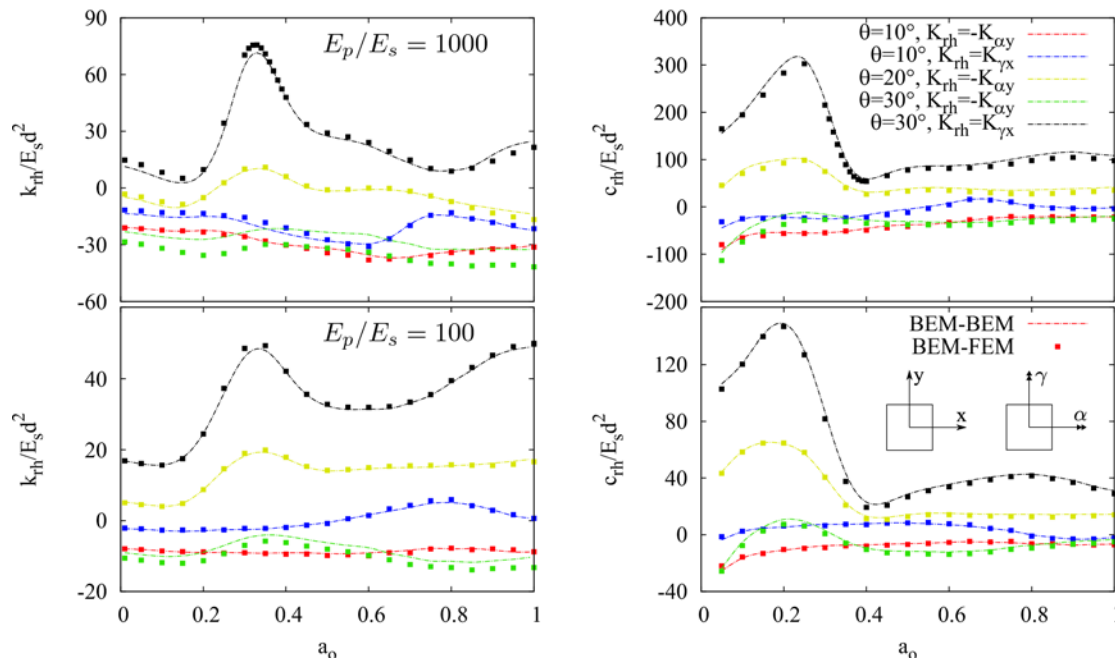


Figure 6. Comparison between horizontal-rocking crossed impedances obtained by BEM-BEM and BEM-FEM models.

## References

- [1] G. Gazetas and G. Mylonakis. Seismic soil-structure interaction: new evidence and emerging issues. In *Geotechnical Earthquake Engineering and Soil Dynamics III ASCE, Geotechnical Special Publication II*, 1119-1174 (1998).
- [2] J. Guin. Advances in soil-pile-structure interaction and non-linear pile behavior, *Ph.D. Thesis, State University of New York at Buffalo* (1997)
- [3] N. Gerolymos, A. Giannakou, I. Anastasopoulos and G. Gazetas. Evidence of beneficial role of inclined piles: observations and summary of numerical analyses. *Bulletin of Earthquake Engineering*, **6**(4),705-722 (2008)
- [4] A. Giannakou, N. Gerolymos, G. Gazetas, T. Tazoh and I. Anastasopoulos. Seismic behavior of batter piles – I. Elastic Response. *Journal of Geotechnical and Geoenvironmental Engineering, ASCE, In Press* (2010)
- [5] S.M. Mamoon, A.M. Kaynia and P.K. Banerjee. Frequency domain dynamic analysis of piles and pile groups. *J Eng Mech ASCE*, **116**, 2237-2257 (1990)
- [6] L.A. Padrón, J.J. Aznárez and O. Maeso. BEM-FEM coupling model for the dynamic analysis of piles and pile groups. *Engineering Analysis with Boundary Elements*, **31**, 473-484 (2007)
- [7] L. A. Padrón. Numerical model for the dynamic analysis of pile foundations, *Ph. D. Thesis, University of Las Palmas de Gran Canaria* (2009) (available for download at <http://hdl.handle.net/10553/2841>)
- [8] J. Domínguez. Boundary Elements in Dynamics. *Computational Mechanics Publications & Elsevier Applied Science, Southampton, NY* (1993)
- [9] O. Maeso, J.J. Aznárez and F. García. Dynamic impedances of piles and groups of piles in saturated soils. *Computers and Structures*, **83**, 769-782 (2005)
- [10] F. Vinciprova, O. Maeso, J.J. Aznárez and G. Oliveto. Interaction of BEM analysis and experimental testing on pile-soil systems. In *Problems in structural identification and diagnostic: General aspects and applications*. Springer-Verlag, 195-227 (2003)